Received: 29 January 2024 | Revised: 28 May 2024 | Accepted: 27 June 2024

DOI: 10.1049/itr2.12537

IET Intelligent Transport Systems

The Institution of Engineering and Technology WILEY

ORIGINAL RESEARCH

A simulation-based impact assessment of autonomous vehicles in urban networks

Hashmatullah Sadid | **Constantinos Antoniou**

Technical University of Munich (TUM), TUM School of Engineering and Design, Chair of Transportation Systems Engineering, Munich, Germany

Correspondence
Hashmatullah Sadid, Technical University of Munich (TUM), TUM School of Engineering and Design, Chair of Transportation Systems Engineering, Munich, Germany.
Email: hashmat.sadid@tum.de

Funding information
Deutscher Akademischer Austauschdienst; Research Grants - Doctoral Programmes in Germany

Abstract

The behavioural differences between autonomous vehicles (AVs) and human-driven vehicles (HDVs) can significantly impact traffic efficiency, safety, and emissions. Simulation-based impact assessments using microscopic traffic models often modify car-following (CF) and lane-changing (LC) configurations to differentiate AVs from HDVs. Typically, researchers adjust CF model parameters to replicate AV driving behaviour, but these assumptions can lead to varying conclusions on AV impacts. The scope of each study (e.g., freeways, highways, urban links, intersections) also influences the outcomes. This research conducts an impact assessment utilizing optimized AV driving behavior rather than assumptions on a city network level (Munich) using a simulation-based platform. The particle swarm optimization (PSO) algorithm is used to calibrate the base model and run simulation experiments under various penetration rates (PRs) and demand scenarios. Results show significant safety improvements throughout the network under higher PRs, while lower PRs might lead to deteriorating safety. At 100% AV PR, the total number of conflicts decreased by around 25% compared to a fully HDV environment. Considering AVs' sensing capabilities, additional safety improvements are found in almost any AV PR. However, AVs might not improve traffic efficiency; in some cases, they may slightly increase average network travel time, though this change is minimal.

1 | INTRODUCTION

Fully automated vehicles, also called autonomous or self-driving vehicles, will gradually enter the market. There are optimistic and pessimistic views about the mass deployment of autonomous vehicles (AVs). From an optimistic perspective, predictions are toward significant impacts of AVs on traffic safety improvement [1, 2], congestion reduction [3], fuel savings [4–6], vehicle emissions reduction [5], and driving restrictions [7, 8]. On the other hand, the pessimistic view challenges the penetration of AVs on the market due to their potential technical failures [9, 10], social acceptance [11], costs [12], induced traffic demand [13], years of testing, and regulatory approvals. Since new technological innovations have rapidly entered the market, it is expected that AVs might experience the same trend. We will eventually witness a situation where AVs interact with human-driven vehicles (HDVs), cyclists, and pedestrians [14].

From a transportation perspective, AVs might have different driving behaviour than HDVs. These differences are due to AVs' sensing and communication capabilities. AVs can detect the precise picture of the surrounding environment using advanced sensing technologies (e.g. radar and lidar) and react accordingly with the help of a trained decision processing unit (DPU). Meanwhile, AVs are capable of exchanging driving status (i.e. speed, acceleration, position, and more) with other connected vehicles and infrastructure (thanks to V2V and V2I), which are labelled as connected autonomous vehicles (CAVs) [15, 16].

AVs and CAVs are expected to bring significant changes in mobility, safety, and emissions. Many researchers have conducted simulation-based studies to quantify these potential changes in transportation systems. Microscopic traffic models (MTMs) are widely used to predict the impact of AVs and CAVs on safety and efficiency. The general findings of most studies reveal that higher penetration rates (PRs) of AVs and/or CAVs could have more considerable impacts on efficiency and safety [17–23]. More optimistic views are for CAVs in comparison to AVs [22, 24–26]. However, the magnitude of changes differs among various studies. It is also reported that higher demands for CAVs could lead to substantial changes in the network [25, 27]. In contrast, some studies reported different findings on the impacts of AVs and CAVs. For instance, [26] reported that compared to HDVs and with the constant demand, any PRs of AVs do not improve the traffic flow efficiency; however, CAVs enhance the condition. They also reported that in lower traffic demands, HDVs always outperform CAVs.

To design an experimental setup for evaluating the impacts of AVs deployment scenarios, replicating the AVs' driving behaviour is crucial. In MTMs, the driving behaviour of vehicles is modelled both in terms of their longitudinal (car-following) and lateral (lane-changing) configurations. Several studies have attempted to approximate the accurate characteristics of these behaviours (especially CF behaviour) for AVs and CAVs in MTMs [17, 22, 28–30]. Although there are many state-of-the-art modelling methods for the CF behaviour of AVs and CAVs, they require defining a certain set of parameters. The values of these parameters are often based on assumptions or estimated using limited trajectory data from field experiments involving AVs and CAVs. The use of various CF models with researchers' assumptions for model parameters leads to different findings regarding the impacts of AV deployment scenarios. To address this challenge, two possible solutions could be employed: first, utilization of mass real-world AV data to calibrate a specific CF model; second, use the optimal driving behaviour of AVs and extract the optimized parameters of a CF model. By adopting either of these approaches, researchers can ensure a more accurate replication of AV driving behaviour in MTMs, leading to more reliable evaluations of AV deployment scenarios.

The first approach, which involves the utilization of mass real-world AV data to calibrate a CF model, faces significant challenges due to the lack of extensive field data for AVs. The available data are often limited to specific locations and driving behaviours, making them non-generalizable. Therefore, the second approach, involving the optimization of AV driving behaviour and extraction of optimized CF model parameters, could be more feasible and effective in MTMs for mimicking the driving behaviour of AVs.

It is expected that the DPU of the AVs contains pre-trained complex deep learning algorithms that regulate the AV to react in any traffic situation while keeping safe and efficient driving manoeuvres [31]. In MTMs, we can regulate AVs to generate optimal trajectories from origin to destination, considering all driving constraints. A CF model that generates such an optimal driving manoeuvre for AVs is referred to as optimized CF behaviour. In our previous work in [31], we developed a framework that finds a set of optimized driving parameters of AVs under various PRs, demand scale, and optimization functions. The extracted optimized CF behaviour could be used in a simulation-based impact assessment study to give more realistic results on the potential impacts of AVs rather than weak assumptions. Hence, the main aim of this research is to investigate the impacts of AVs on mobility and safety using the optimal driving behaviour of AVs. Furthermore, most AV impact assessment studies focus on intersections [17, 32], urban links [18, 19, 33], and freeways [22, 27, 34–36], whereas limited studies are conducted at the network level; therefore, our research focuses on impact assessment in a traffic network.

The main contributions of this research are: (i) to assess the potential impacts of AVs deployment scenarios in a traffic network, and (ii) to study the influencing factors on the potential impacts of AVs using generalized estimating equation (GEE) and zero-truncated Poisson (ZTP) regression models. This paper investigates how the behavioural difference of AVs with optimized driving behaviour could bring changes on the efficiency and safety of a network, where other factors, such as infrastructure, speed limit, intersection controllers, and more, play a vital role in the performance of traffic flow and safety.

The remainder of this paper is structured as follows. In the following section, we review the recent literature on microscopic simulation tools utilized for AVs impact assessment. In Section 3, we introduce the methodology of this research, including a calibration scheme, the modelling method for replicating AVs' longitudinal driving behaviour, the evaluation areas, and the design of an experimental setup. The experimental setup aims to run different AVs deployment scenarios in a city-scale network with calibrated and validated features. The findings of this research and the results of regression analysis (run on achieved results) are presented in Section 4, which is followed by a discussion in Section 5. Finally, a conclusion in Section 6 explains the overall contribution of this article alongside further research directions.

2 | LITERATURE REVIEW

A wide range of simulation-based studies focus on identifying the potential impacts of AVs on the transportation system. In a simulation-based study, three aspects are essential for setting up an experiment and conducting impact assessment, namely (i) the calibration of the base model, and the selection of an appropriate CF model, including the adopted parameters to replicate the driving behaviour of AVs, (ii) defining the assessment areas and key performance indicators (KPIs) to quantify the impacts, and (iii) the choice of a powerful traffic simulation tool. In the following subsections, we present each aspect in detail.

2.1 | Modelling and calibration of the car following behaviour

CF models play a crucial role in MTMs and simulation tools. These models describe how individual vehicles behave while following each other on roads, considering factors like speed, distance, acceleration, and reaction to changes in the environment. Replication of vehicular CF behaviour has been a continuous research focus in the field of traffic modelling and simulation. CF models are generally categorized into mathematical and data-driven models. Mathematical models rely on fundamental principles of physics and mathematics to describe how vehicles interact with each other on the road under different traffic situations. On the other hand, data-driven models are developed directly from observed data on vehicle trajectories and behaviour collected from real-world traffic conditions. These models use statistical techniques and machine learning algorithms to analyse patterns in the data and develop mathematical representations of typical CF behaviour. Although data-driven models outperform many mathematical models in replicating the CF behaviour of vehicles, they are not widely used in impact assessment studies.

Mathematical models are initially developed to replicate the driving behaviour of HDVs and have been widely used in simulation tools. These models comprise methods focusing on a driver's physical actions, such as desired speed, acceleration, deceleration, i.e. Gazis–Herman–Rothery (GHR) model [37], Gipps model [38], intelligent driver model (IDM) [39], optimal velocity model (OVM) [40]; however, some also consider the psychological inputs of the drivers, such as the Wiedemann model [41]. These models are comprised of modifiable parameters that mimic the driving behaviour and are often calibrated with mass field driving data of vehicles. The behavioural calibration of a CF model involves the fine-tuning of its modifiable parameters to minimize the discrepancies between real-world driving configurations and the simulated environment. Several methods have been implemented to calibrate a CF model in the literature. These methods include genetic algorithm (GA) [42–47], particle swarm optimization (PSO) [48, 49], machine learning-based methods [50], and combination of various optimization techniques [51, 52]. For instance, [42] employed the GA to calibrate the parameters of IDM, Gipps, Wiedemann, GHR, and FVD (full velocity difference) [53] models. [49] used the PSO algorithm to extract the calibrated parameters of a psychophysical CF model in a microsimulation. Meanwhile, [50] implemented an artificial neural network (ANN)-based model to calibrate the parameters of the Wiedemann model. On the other hand, [51] proposed the combination of the PSO and machine learning-based approach to calibrate the default CF model of the Transmodeler simulation tool. Given that this research conducts impact assessment of AVs deployment scenarios in mixed traffic, we need to calibrate the base model (fully HDVs environment) to accurately approximate the driving behaviour of HDVs in real-world traffic conditions. Hence, in this research, we employ PSO for behavioural calibration.

Furthermore, for AVs, there are no established mathematical models, and researchers often employ conventional mathematical models to mimic the CF behaviour of AVs. According to [54], IDM, MIXIC, Wiedemann 99, and Krauss models are frequently used CF models for mimicking the driving behaviour of AVs in literature. The selection of a specific CF model for replicating the driving behaviour of AVs in simulation-based impact assessment studies depends first on whether the model can replicate the potential driving behaviour of AVs and second on whether it is well-integrated in a widely used simulation tool. For instance, Wiedemann 99 is the default CF model of VISSIM; therefore, many studies utilized Wiedemann 99 to mimic the CF behaviour of AVs and conduct impact assessment using VISSIM. An overview of the simulation tools and their CF models is presented in Section 2.3.

Given the current impracticality of large-scale AV testing and the limitations of available AV-related data, which are restricted to specific locations and driving behaviours, accurately calibrating a CF model to replicate AV driving behaviour is not feasible. Consequently, impact assessment studies often rely on the assumed driving behaviours of AVs. Some studies assume AVs will drive more cautiously with larger headway gaps, while others assume a more aggressive driving style. These differing assumptions lead to conflicting findings, particularly regarding the number of conflicts and overall safety. In contrast, this research employs the optimal driving behaviour of AVs to conduct network-wide impact assessment [54].

2.2 | Assessment areas and KPIs

In simulation-based impact assessment, the selection of assessment areas and their relevant KPIs is important for constructing an effective experimental setup. These choices ensure that the simulation can comprehensively evaluate the potential impacts of AVs across various dimensions. A review of previous studies reveals that the majority of researchers conduct impact assessments of AVs and CAVs for safety and traffic efficiency, where some also evaluate the environmental effects (e.g. energy consumption and emissions) [54]. For each assessment area, various KPIs are chosen depending on the scope of the study. For efficiency assessment, most researchers employed KPIs such as traffic flow (e.g. traffic flow, density), average travel time, string stability, average velocity, and more [22, 29, 30, 34]. For instance, [18] studied the impact of CACC-equipped vehicles on traffic efficiency in urban roads with congested sections. This study selects traffic capacity, waiting time, queue length, and total travel time as the main KPIs. The findings of this study indicate that in comparison to conventional vehicles, CACC-equipped vehicles with a PR of 100% can increase the traffic capacity by more than 2.6 times. The study claims that by increasing the PR of CACC-equipped vehicles, the waiting time on congested roads decreases.

Similarly, for safety evaluation, researchers use the surrogate safety measure (SSM) model to quantify the potential conflicting situations and to assess the impact of AVs PRs on traffic safety. Most studies used time-to-collision (TTC), post-encroachment time (PET), and number of conflicts (using certain TTC and PET thresholds) as KPIs for safety assessment in the literature [17, 22, 28, 55]. A recent study by [28] explored the impacts of CAVs on the safety of a motorway section. In this study, the number of conflicts is used as a KPI. The results revealed that higher PRs of CAVs reduce traffic conflicts. Similarly, [17] investigated the effects of CAVs on the safety of signalized and unsignalized intersections. The findings of this study showed that CAVs can significantly reduce the number of conflicts at both intersections. In addition, it is claimed that a 100% PR of CAVs could eliminate any crossing conflicts between vehicles.

Finally, for emission assessment, the amount of CO_2 and NOx emissions per kilometres g/kg are used as KPIs [24, 25].

One important note is that most studies assume the same energy consumption and emissions factors used for existing HDVs and for AVs. [25] conducted a simulation-based study to investigate the impact of (C)AVs on throughput and emissions in a ring road. CO_2 and emissions per kilometre are selected as KPIs for environmental impacts. The findings of this study highlighted that in free-flow traffic, where vehicles are not bound to speed limits, human-driven vehicles exhibit the highest emissions. Conversely, any PRs of CAVs could lead to low emissions. The study also claimed that AVs drive at low speeds and thus force the engine to work less efficiently. Hence, in comparison to CAVs, AVs increase emissions.

2.3 | Microscopic traffic simulators

Microscopic traffic simulators are highly detailed and complex tools that capture the driving behaviour of a single vehicle, including following behaviour, lane change behaviour, and its interaction with other road users. Given the availability of numerous traffic simulators in the market, each with its features and functionalities, it is vital to have a comprehensive understanding of these characteristics. Generally, microscopic traffic simulators are divided into commercial and open-source tools. Commercial traffic simulators are generally user-friendly and less complex products that offer a wide range of user support. Open-source simulators, in comparison, are typically free to use, open, and collaborative, while they have limited user support and are complex for new users. Among many traffic simulators (i.e. VISSIM, AIMSUN, PARAMICS, CORSIM, SUMO), PTV VISSIM, and AIMSUN are the commonly used commercial tools for modelling and simulation of AVs, where SUMO is the open-sources simulator for this purpose.

PTV VISSIM is a multi-modal traffic simulator developed by PTV Group in Karlsruhe, Germany [56]. This widely used tool includes simulating individual vehicles, public transport, bikes, and pedestrians based on the driving behaviour models, control devices, and road network characteristics. VISSIM employs the Wiedemann psychological model [41] to mimic the CF behaviour of vehicles. Modifying the model's parameters allows us to replicate AVs' driving behaviour and conduct impact assessment. The parameters of this model have already been extracted within the CoEXist project to capture the driving behaviour of AVs; however, the calibration of these parameters is based on a few AVs trajectories [57]. VISSIM also gives the option to override the default CF model and control the driving behaviour of AVs externally through the COM interface. The COM interface allows user-developed applications to access network topology, signal control, path flows, and vehicle behaviour. This enables VISSIM to model intricate control logic and advanced transportation systems and components. In addition, the output module of VISSIM enables users to gather a wide range of simulation outputs, including link, node, and network-level traffic data.

AIMSUN (advanced interactive microscopic simulator for urban and non-urban networks), developed by AIMSUN Inc., is a powerful simulation tool allowing both microscopic and mesoscopic simulation capabilities [58]. It offers various tools for traffic demand modelling, network calibration, and performance analysis. AIMSUN Next is well-known for modelling traffic dynamic assignments, incident management, and other ITS applications. AIMSUN Next has the flexibility to model the detailed driving behaviour of vehicles in its microscopic model, which makes it a good candidate for replicating the driving behaviour of AVs. AIMSUN Next supports modelling various modes, including private vehicles, public transport, pedestrian, and bicycles. The default CF model of AIMSUN Next is based on the Gipps' safety distance model [38]. In addition, AIMSUN Next can be further extended with Python scripts, allowing it to automate the simulation with different scenarios, including CF parameter adjustments. The external agent interface (EAI) makes it possible to override the controlling logic of vehicles in the simulation environment both for HDVs and AVs.

SUMO (simulation of urban mobility) developed by German Aerospace (DLR), is an open-source and highly portable microscopic traffic simulation tool [59]. It allows the design and simulation of large-scale networks with detailed vehicular behaviour, including CF, LC, and interactions with traffic controllers and other vehicles. SUMO is widely used in academia for its flexibility, extensibility, and availability of various traffic demand scenario generation tools. In SUMO, each vehicle is modelled explicitly with its own route and runs individually through the network. Several modules, each with its unique function like NETEDIT, TraCi (traffic control interface), SUMO-GUI, routing algorithms, visualization, network import and emission calculation, and more, make SUMO a powerful simulation tool. Regarding CF models, SUMO contains most of the widely used mathematical CF models, including Krauss [60], IDM [39], Gipps [38], and Wiedemann [41] models. SUMO also provides the possibility to model ACC (adaptive cruise control) [61] and CACC (cooperative ACC) [62] equipped vehicles. For the simulation of AVs, researchers either modify the parameters of the available CF model or override any CF logic externally using SUMO's API. Additionally, a mesoscopic simulation mode has been added to SUMO. This mode allows running simulations with less detailed precision, i.e. potentially sacrificing some modelling accuracy, but significantly speeding up the process and reducing computational requirements. This feature enables e.g. the option to initially run numerous scenarios to find a rough optimal solution for a specific problem before utilizing the microscopic version for the final series of runs.

Table 1 provides a summary of different characteristics of the traffic simulators. All three tools simulate traffic in a continuous manner and can replicate AVs driving behaviour by modifying the parameters of the CF models. VISSIM and AIMSUN are user-friendly tools with strong visualization capabilities, but they are commercial, and therefore, their widespread usage in academia is limited. In contrast, SUMO is relatively complex; however, it has high flexibility in generating different scenarios. In addition, since it is open-source, it is a suitable option for various applications, particularly in AVs impact assessment.

TABLE 1 The comparison of widely used traffic simulation tools for AVs modelling.

Criteria/Tool	VISSIM	AIMSUN	SUMO
License	Commercial	Commercial	Open-source
Developer	PTV group	Aimsun Inc.	SUMO Community & DLR Institute
Simulation level	Microscopic	Micro/mesoscopic	Micro/mesoscopic
Visualization	2D and 3D	2D and 3D	2D
Customization	Highly customizable	Customizable	Extensible through plugins and scripting
Supported languages	C++, Java, Python	C++, Java, Python	Python, any programming language for XML config
GUI support	High	Moderate	Moderate
Complexity	Simple	Moderate	Complex
CF models	Wiedemann (74 and 99)	Gipps	Krauss (default), IDM, Gipps, Wiedemann (74 and 99), ACC, and CACC
Modelling of AVs	Customizable to simulate AV behaviour	Supports AV behaviour modelling	Customizable to simulate AV behaviour

Meanwhile, the findings of the literature review show that all three tools are widely used in AV impact assessment studies. The scope of each study in these simulation tools differs from intersections, links to part of a network, as well as freeways. Recent researches, such as [26, 29, 32, 35, 55], utilized PTV VISSIM to evaluate the potential impacts of AV deployment scenarios on traffic efficiency and safety. For instance, [29] investigated the impacts of ACC and CACC-equipped vehicles on traffic efficiency and energy consumption in an ideal expressway. In their research, the MIXIC (microscopic model for simulation of intelligent cruise control) model was used to mimic the driving behaviour of ACC and CACC vehicles in VISSIM. In addition, [35] studied the impacts of AV deployment scenarios on the capacity of a freeway in VISSIM. They utilized the Krauss model to mimic the driving behaviour of AVs by overriding the default Wiedemann model using the COM interface. Similarly, [55] studied the impact of CAV PRs on safety in a Motorway in VISSIM using the default Wiedemann 99 model. Other studies, including [22, 26, 28, 30] used AIMSUN for AVs impact assessment. [28] and [30] used the default Gipps model in AIMSUN to evaluate the safety and efficiency impacts of AVs, respectively. Meanwhile, [22] and [26] used IDM and CACC models in AIMSUN, respectively, by overriding the default CF model to assess the impacts of AV PRs. Finally, many studies also used SUMO for AVs impact assessment [17, 21, 23, 33, 34, 63]. For example, [17] used Krauss, IDM, and CACC models in SUMO to investigate the effects of CAVs on the safety of signalized and un-signalized intersections. [34] studied the impacts of commercially available ACC vehicles on traffic stability and throughput in SUMO. This study used IDM to capture the CF behaviour of theoretical ACC and commercially available ACC vehicles.

In Table 2, the summary of reviewed simulation-based studies is presented, which explains specific information on the CF model, assessment criteria, KPIs, network type, and simulation tools. The table is sorted based on the publication date of the citations, which are displayed in reverse chronological order (newest to oldest).

3 | METHODOLOGICAL FRAMEWORK

3.1 | Approach

In this research, we develop a framework to systematically model and simulate the CF behaviour of AVs under different PRs and conduct a network-wide impact assessment under various demand scenarios. The framework is comprised of three components, namely, a scenario generation module, a simulation environment, and an output module. In the scenario generation module, the corresponding optimized CF parameters are passed into the simulation environment for a certain PR of AVs. There, AVs behave according to these optimized parameters' settings. Since it is expected that AVs might have different driving behaviour than HDVs, the magnitude of these differences might also vary depending on the PR. For instance, AVs might behave similar to HDVs in lower PRs, whereas in higher PRs, their behaviour may be significantly different. Therefore, our framework models AVs with different CF parameter settings depending on the PRs of AVs. The optimized CF parameters' settings under various PRs are extracted using the proposed optimization framework in [31]. Meanwhile, the simulation environment runs multiple simulation replications under the set conditions and outputs the predefined assessment criteria. The output data are further analysed to investigate the potential impacts of AVs. A schematic diagram of the main methodology of this research is depicted in Figure 1. Additionally, for ease of reference, a list of symbols used in the following subsections is provided in Table 3.

3.2 | Modelling CF behaviour of human-driven vehicles

In this research, we choose IDM to replicate the CF behaviour of HDVs since it has been widely used in the literature to accurately replicate drivers' driving behaviour. IDM, first developed

TABLE 2 Summary of reviewed simulation-based studies on AVs including their CF model, assessment criteria, KPIs, network type, and traffic simulator.

Reference	Year	CF model	Assessment criteria	KPIs	Network	Simulator
[28]	2023	Gipps	Traffic safety	Number of conflicts	Freeway	AIMSUN
[29]	2023	MIXIC	Traffic efficiency and energy consumption	Average travel time, capacity, average electric energy consumption	Expressway	VISSIM
[17]	2022	Krauss, IDM, and CACC	Traffic safety	Number of conflicts	Intersection	SUMO
[30]	2022	Gipps	Capacity analysis	Network capacity	City	AIMSUN
[22]	2021	IDM	Traffic safety and efficiency	Time-to-collision (TTC), number of conflicts, travel time	Freeway	AIMSUN
[34]	2021	IDM	Throughput and stability	Traffic flow, density	Freeway	SUMO
[18]	2021	CACC	Traffic efficiency	Traffic flow, density, critical speed	Urban road	Numerical simulator
[21]	2021	Krauss	Traffic efficiency	Traffic flow, travel time	City	SUMO
[35]	2020	Krauss	Capacity analysis	String stability, lane capacity	Freeway	VISSIM
[23]	2020	IDM	Traffic efficiency	Travel time	Freeway	SUMO
[63]	2020	Krauss	Capacity analysis	Speed, flow, density	Urban road	SUMO
[55]	2019	Wiedemann 99	Safety analysis	Number of conflicts	Motorway	VISSIM
[26]	2018	CACC	Throughput	Harmonic average speed	Ring road	AIMSUN
[64]	2018	Wiedemann 99	Traffic safety	Number of conflicts	Roundabout	VISSIM
[32]	2018	Wiedemann 99	Safety analysis	Number of conflicts	Signalized intersection and roundabout	VISSIM
[33]	2018	Krauss	Capacity analysis	Flow, density	Grid network	SUMO
[65]	2016	Wiedemann 99	Traffic efficiency	Average density, travel time, and speed	Autobahn	VISSIM

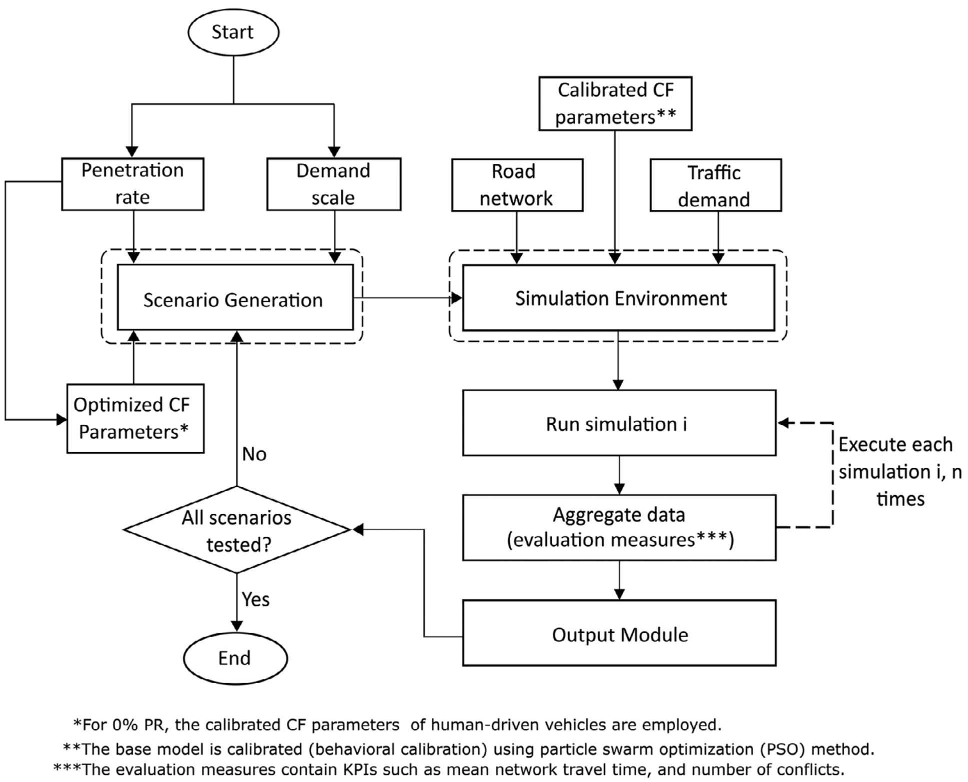

FIGURE 1 The methodological framework in this study.

TABLE 3 The list of symbols used in this research.

Category	Symbol	Description
IDM	$a_n(t)$	Acceleration of vehicle n
	$a_{\max}$	Maximum acceleration/deceleration of the vehicle
	V_n, $V_0^{(n)}$	Speed, and desired speed of the following vehicle
	S_n	The gap distance between two vehicles
	S_n^*	Desired spacing between two vehicles
	δ	Model parameter
	ΔV_n	Speed difference between following and leading vehicles
	$S_0^{(n)}$	Minimum spacing at a standstill situation
	T_n	Desired (safe) time headway
	$b^{(n)}$	Desired (comfortable) deceleration
Krauss	v_{safe}	Safe velocity of the following vehicle
	v_{l}	Speed of the leading vehicle
	v_{f}	Speed of the following vehicle
	t_{r}	Reaction time of the driver
	b	Maximum comfort deceleration
	$g(t)$	Gap between the leading and the following vehicles
	x_{l}	Position of the leading vehicle
	x_{f}	Position of the following vehicle
	L	Average length of a vehicle
	v_{des}	Desired speed of the following vehicle
GEE	K	Number of clusters
	n_i	Observations in cluster i
	Y_{ij}	Response for jth observation in cluster i
	X_{ij}	Covariate vector for jth observation in cluster i
	μ_{ij}	Mean for jth observation in cluster i
	β	Regression coefficients
	$R_i(\alpha)$	Working correlation matrix for cluster i
	α	Correlation parameter
	ϕ	Scale parameter
ZTP	y	Observed count in a time interval
	λ	Mean parameter of the Poisson distribution
	$E(y)$	Expected count
	$\text{Var}(y)$	Variance
	$g(\lambda)$	Link function in the ZTP regression model
	$\hat{\lambda}$	Estimated mean parameter
	$\mathbf{X}$	Design matrix
	β	Vector of regression coefficients
	ϵ	Random error with a standard logistic distribution

by [39], is one of the simplest and accident-free models, which utilizes both the desired speed and space headway to generate a realistic acceleration profile. The basic form of the IDM acceleration function is expressed as:

$$a_n(t) = a_{\max}^{(n)}\left[1 - \left(\frac{V_n(t)}{V_0^{(n)}(t)}\right)^{\delta} - \left(\frac{S_n^*(t)}{S_n}\right)^2\right] \tag{1}$$

where $a_{\max}$ represents the maximum acceleration or deceleration of the vehicle n, V_n is the speed of the following vehicle, $V_0^{(n)}$ is the desired speed of the following vehicle, S_n is the gap distance between two vehicles, S_n^* is the desired spacing between two vehicles, and δ denotes the model parameter. The desired space headway between two vehicles S_n^* is a function of the following vehicle speed V_n and the speed difference between the leading and following vehicles ΔV_n, which can be estimated as follows:

$$S_n^*(t) = S_0^{(n)} + V_n(t)T_n(t) + \frac{V_n(t)\Delta V_n(t)}{2\sqrt{a_{\max}^{(n)} b^{(n)}}} \tag{2}$$

where $S_0^{(n)}$ is the minimum spacing at a standstill situation, T_n is the desired (safe) time headway, and $b^{(n)}$ is the desired (comfortable) deceleration.

The IDM model parameters are calibrated (behavioural calibration) based on the real-field travel time data. Since we utilize a dynamic traffic assignment-based simulation model in SUMO, the route choice is already calibrated in another study employing the same demand and network characteristics [66]. Thus, we only conduct behavioural calibration to match the simulated travel times with the real-field travel times of links in the network, keeping the traffic assignments unchanged. The data include the peak-hour travel time information along several major roads in Munich city center network. This research uses the PSO algorithm to calibrate the IDM parameters. PSO is a metaheuristic, stochastic, and population-based optimization algorithm inspired by the behaviour of bird flocking or fish schooling. It is used to find the global optimal solution by iteratively updating a population of candidate solutions (particles) in a search space [67]. The algorithm iteratively searches for the design space to improve a candidate solution with regard to an objective function. Unlike gradient-based optimization methods, PSO does not require the objective function to be differentiable, divisible, and continuous. The choice of PSO in this research is associated with its convergence speed and computational efficiency [68, 69].

In PSO, each particle represents a candidate solution and moves through the search space by adjusting its position based on its own experience and the collective knowledge of the entire population. The particles' movements are influenced by two key factors: their own best-known status (pbest) and the best-known position of the whole population (known as gbest) [70]. By incorporating these references, particles are directed toward regions of the search space that exhibit promising solutions,

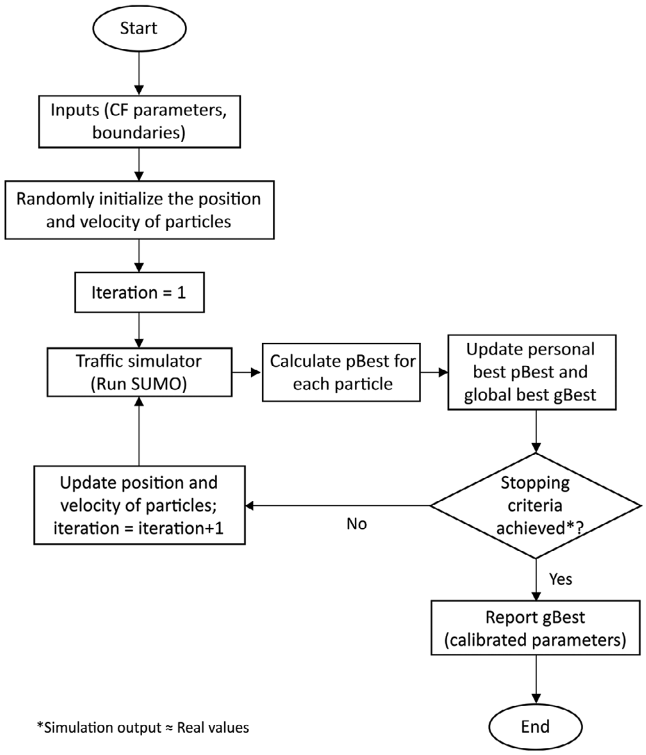

FIGURE 2 Illustration of PSO calibration method.

allowing for effective exploration and exploitation during optimization. This paper uses the root mean square normalized (RMSN) as an objective function to minimize the dispersion between the simulated and true travel times, where the input variables are the CF model parameters. PSO tries to change the parameters of the CF model within their boundary conditions (i.e. realistic driving behaviour, acceleration and deceleration capability, comfort driving etc.), aiming to find the minimum RMSN. The overall process of the PSO algorithm integrated with SUMO traffic simulator is illustrated in Figure 2.

3.3 | Modelling CF behaviour of AVs

In this research, we utilize the Krauss CF model to replicate the longitudinal driving behaviour of AVs. This model is widely used in modelling the CF behaviour of AVs in MTMs, and is the default CF model in SUMO. The Krauss CF model developed by Stephan Krauss in 1997 is a space-continuous model [60].

TABLE 4 Krauss model's optimized AV parameters [31].

PRs [%]	Mingap [m]	Accel [m/s^2]	Decel [m/s^2]	Sigma [-]	Tau [s]
20	1.6	2.6	3.6	0.4	0.8
40	1.5	2.7	3.7	0.4	0.8
60	1.1	3.4	3.2	0.1	1.0
80	1.2	3.0	3.4	0.4	1.0
100	1.3	2.5	3.6	0.5	1.0

(Sigma = driving imperfection factor, Tau = desired time headway).

Krauss model estimates the safe speed of the vehicle without deriving it from the acceleration profile of the vehicle. In Krauss model, the safe velocity of the following vehicle is calculated as follows:

$$v_{\mathrm{safe}}(t) = v_{\mathrm{l}}(t) + \frac{g(t) - v_{\mathrm{l}} \cdot t_{\mathrm{r}}}{\frac{v_{\mathrm{l}}(t)+v_{\mathrm{f}}(t)}{2b} + t_{\mathrm{r}}} \tag{3}$$

where v_{l}, v_{f} are the speed of leading and following vehicles at time t respectively (see Figure 3), t_{r} is the reaction time of the driver, b is the maximum comfort deceleration of the vehicle, and $g(t)$ is the gap between the following and leading vehicles, which is computed as: $g(t) = x_{\mathrm{l}}(t) - x_{\mathrm{f}}(t) - L$, ($x_{\mathrm{l}}$, x_{f} are the position of the leading and following vehicles, and L is the average length of a vehicle).

Meanwhile, to estimate the desired speed, which is a decisive variable for determining the speed of the vehicle in the next time step, the model takes the minimum of safe velocity, the road speed limit, and the vehicle's maximum capable speed to generate the desired speed of the vehicles, expressed as:

$$v_{\mathrm{des}}(t) = \min[v_{\mathrm{max}}, v(t) + a \cdot \Delta t, v_{\mathrm{safe}}(t)] \tag{4}$$

Finally, the velocity and location of the vehicle at the next time step are computed as follows:

$$\begin{aligned} v(t+\Delta t) &= \max[0, v_{\mathrm{des}}(t) - \eta], \\ x_f(t+\Delta t) &= x_{\mathrm{f}}(t) + v(t+\Delta t) \cdot \Delta t \end{aligned} \tag{5}$$

where η is the random perturbation (to capture the driving imperfection) and Δt is the simulation time step. The optimized parameter of the Krauss CF model was already extracted in [31] as depicted in Table 4.

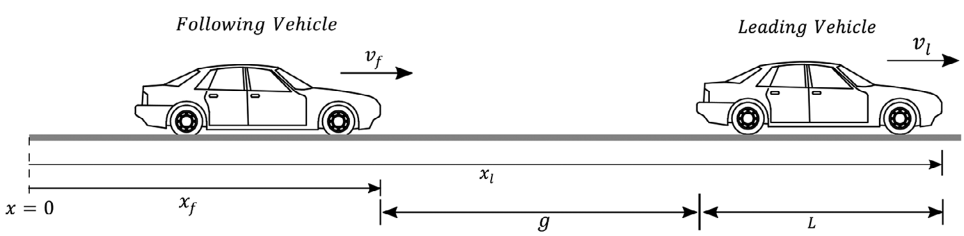

FIGURE 3 Description of the Krauss CF model parameters.

3.4 | Evaluation areas

In this research, we select traffic efficiency and safety as evaluation areas to estimate the impacts of AVs deployment scenarios on transport network performance. Traffic data, including edge-related, intersection-level, and network-wide information, are collected for the evaluation of efficiency. For safety assessment, we utilize the surrogate safety measure (SSM).

3.4.1 | Traffic efficiency assessment

Traffic data is collected from the simulation environment in 5-min intervals for each link, intersection, and overall network. Depending on the assessment criteria, we utilize various KPIs, such as travel time, flow, occupancy, speed, density, time loss, and queue length, for traffic efficiency analysis. To make sure the outputs of simulation runs under different AV scenarios are significantly different, we employ a one-way ANOVA (analysis of variance) statistical approach. Meanwhile, to investigate whether each pair of scenarios is different from the other, we apply Tukey's HSD (honestly significant difference) test.

First, we investigate the traffic flow elements (average volume, speed, occupancy, density, average travel time) through specific segments (edges) of the network under various scenarios. The data gathered from the loop detectors installed on edges are further used to study the specific impacts of different AVs scenarios on links. Second, to analyse the effects of AV PRs on the traffic situation of signalized intersections, average passing speed, and average time loss are utilized as KPIs. We collect this information using area detectors around each signalized intersection. Finally, for analysis of the network performance, the average network travel time is calculated under different AV PRs using every vehicle's travel time. For a single vehicle, the travel time is estimated using the difference between the departure and arrival times. Hence, the mean of aggregated travel times of all vehicles in the network corresponds to the average network travel time.

Furthermore, to investigate the relationship between the potential impacts, PRs, and other relevant factors (e.g. flow, speed etc.), we implement the generalized estimating equation (GEE) regression method. GEE is a statistical method that is used for analysing data with correlated or clustered observations. GEE is an extension of generalized linear models (GLMs), which is used in longitudinal studies (repeated observations) and clustered data (data collected from different clusters or groups) [71]. In our case, edge travel time is collected in 5-min intervals during the simulation period. Thus, each edge segment is considered as a cluster, and the repeated observation is the travel time.

Suppose the datasets (travel time) of repeated observations involving K clusters of edges. Each cluster i (where $i = 1, 2, \dots, K$) is associated with n_i observations denoted as response vector Y_{ij} (travel time) of the jth response ($j = 1, 2, \dots, n_i$). Furthermore, let X_{ij} represent a $p \times 1$ vector of explanatory variables (covariates) corresponding to each observation. We can define the response vector for the ith cluster as $Yi = (Y_{i1}, Y_{i2}, \dots, Y_{i(n_i)})$ and its mean vector as $\mu_i = (\mu_{i1}, \mu_{i2}, \dots, \mu_{i(n_i)})$, where μ_{ij} denotes the mean value for the jth response. The means μ_{ij} are related to the p dimensional regression vector X_{ij} by the $p \times n_i$ mean-link function g as follows:

$$g(\mu_{ij}) = X_{ij}^{\top} \cdot \beta \tag{6}$$

where β is the unknown $p \times 1$ vector of regression coefficient with the true value β_0. In addition, let the conditional variance of Y_{ij} given X_{ij} be:

$$\mathrm{Var}(Y_{ij} \mid X_{ij}) = v(\mu_{ij})\phi \tag{7}$$

where v is a known variance function of μ_{ij}, and ϕ is the scale parameter. Both v and ϕ are associated with the distribution of the responses. For instance, in case Y_{ij} follows a Gaussian distribution, μ_{ij} is specified as 1, and if it shows Poisson distribution, then $\mu_{ij} = \mu_{ij}$. Also, let the $R_i(\alpha)$ be the working correlation matrix ($n_i \times n_i$) or the pattern of measures within a cluster which is described by the vector parameter α, then the variance-covariance matrix for Y_i is expressed as:

$$V_i = \phi A_i^{\frac{1}{2}} R_i(\alpha) A_i^{\frac{1}{2}} \tag{8}$$

where $A_i^{\frac{1}{2}}$ is a ($n_i \times n_i$) diagonal matrix with entries $v(\mu_{ij})$ as the jth diagonal element. The GEE for estimation of the ($p \times 1$) β is obtained by solving the following equation:

$$\sum_{i=1}^{K} \frac{\partial \mu_i^{\top}}{\partial \beta} V_i^{-1}(Y_i - \mu_i(\beta)) = 0 \tag{9}$$

where $\frac{\partial \mu_i^{\top}}{\partial \beta}$ is a ($p \times ni$) matrix of the partial derivative of the mean in regard to the regression parameter of the ith cluster, which is obtained as follows:

$$\frac{\partial \mu_i^{\top}}{\partial \beta} = \begin{bmatrix} \frac{x_{i11}}{g'(\mu_{i1})} & \cdots & \frac{x_{ini1}}{g'(\mu_{ini})} \\ \vdots & & \vdots \\ \frac{x_{i1p}}{g'(\mu_{i1})} & \cdots & \frac{x_{inip}}{g'(\mu_{ini})} \end{bmatrix} \tag{10}$$

[71] propose utilizing consistent moment estimates for both parameters, ϕ and α. This results in an iterative process that alternates between estimating β for fixed values of $\hat{\phi}$ and $\hat{\alpha}$, and estimating ϕ and α for fixed values of $\hat{\beta}$. This approach results in a consistent estimate for β. According to [71], this also holds if the working correlation structure $R_i(\alpha)$ is misspecified.

Meanwhile, there are many different structures for working correlation matrix, including independent, exchangeable, k-dependent, autoregressive, Toeplitz, and unstructured; in this paper, we select independent and exchangeable for GEE analysis.

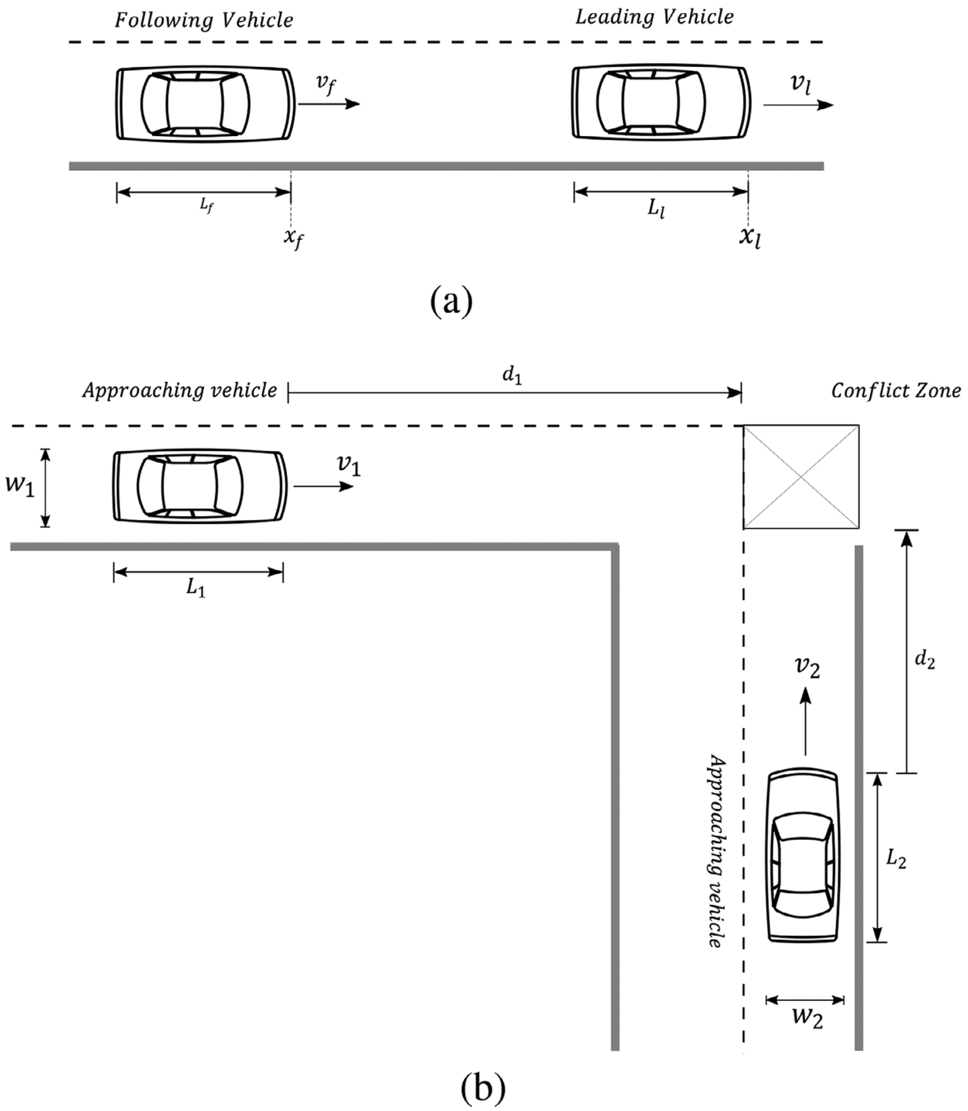

FIGURE 4 Illustration of TTC under (a) follow–lead, and (b) approaching conflicts scenarios.

- Independent R: within a cluster, the observations are independent.

$$\mathrm{Corr}(Y_{ij}, Y_{ik}) = \begin{cases} 1 & j = k \\ 0 & j \neq k \end{cases}, \qquad \text{e.g.} \begin{pmatrix} 1 & 0 & 0 \\ 0 & 1 & 0 \\ 0 & 0 & 1 \end{pmatrix} \tag{11}$$

- Exchangeable R: within a cluster, the observations hold a constant correlation.

$$\mathrm{Corr}(Y_{ij}, Y_{ik}) = \begin{cases} 1 & j = k \\ \alpha & j \neq k \end{cases}, \qquad \text{e.g.} \begin{pmatrix} 1 & \alpha & \alpha \\ \alpha & 1 & \alpha \\ \alpha & \alpha & 1 \end{pmatrix} \tag{12}$$

3.4.2 | Safety assessment

For safety evaluation, the SSM is used to approximate the number of conflicts in the network. For this purpose, each vehicle is equipped with an SSM device, which logs the conflicts of the vehicle with other vehicles. In this research, time-to-collision (TTC) is used for the traffic conflict analysis. TTC is the time required to collide between two vehicles in follow–lead as well as approaching situations. Depending on the scenarios (as depicted in Figure 4), TTC calculation is expressed as:

$$\mathrm{TTC} = \begin{cases} \frac{x_l - x_f - L_f}{v_f - v_l}, & \text{if } v_l > v_f \\ \frac{d_2}{v_2}, & \text{if } \frac{d_1}{v_1} < \frac{d_2}{v_2} < \frac{d_1 + L1 + w1}{v_1} \\ \frac{d_1}{v_1}, & \text{if } \frac{d_2}{v_2} < \frac{d_1}{v_1} < \frac{d_2 + L2 + w2}{v_2} \end{cases} \tag{13}$$

A conflict is considered when the TTC value is less than the specified threshold. A TTC value of 1.5 s or less is considered as unsafe condition; hence, in this research, we set the TTC threshold to 1.5 s. The sum of all conflicts noticed during the simulation period indicates the total number of conflicts in the network. Similarly, we apply the one-way ANOVA statistical approach to check whether the total number of conflicts among scenarios are significantly different. In addition, to investigate whether each pair of scenarios is different from each other, we implement Tukey's HSD test [72].

Meanwhile, since AVs sensing technologies could potentially detect and respond to a conflicting situation much faster than HDVs, the unsafe TTC threshold might be lower for AV-AV and AV-HDV interactions. Hence, we conduct a sensitivity analysis to check how different PRs of AVs affect the total number of conflicts under various TTC thresholds.

Furthermore, to model the relationship between traffic characteristics, PRs, and the total number of conflicts in the network, we utilize a zero truncated Poisson (ZTP) regression model. The ZTP is a statistical approach used for analysing count data, excluding zero values from the dataset [73, 74]. Since this research employ the total number of conflict in the network for analysis, the zero number of conflicts in the network is not practical. The probability mass function (PMF) of the ZTP distribution is expressed as follows:

$$P(y;\lambda) = \frac{\lambda^y}{y!(e^{-\lambda}-1)}, \qquad y = 1, 2, 3, \ldots \tag{14}$$

where y is the observed count in a time interval, and λ is the mean parameter of the Poisson distribution. In addition, the expected counts and the variance for given λ can be expressed as follows:

$$E(y) = \frac{\lambda e^{\lambda}}{e^{\lambda}-1}, \qquad \mathrm{Var}(y) = \frac{\lambda e^{\lambda}}{e^{\lambda}-1}\left(1 - \frac{\lambda}{e^{\lambda}-1}\right) \tag{15}$$

Finally, the ZTP regression model (link function) is as follows:

$$g(\lambda) = \log(\hat{\lambda}) = \mathbf{X}\beta + \epsilon \tag{16}$$

where X is the design matrix, β is the vector of regression coefficients, and ϵ is the random error that has the standard logistic distribution. In this model, we take different PRs of AVs, the standard deviation of the average network speed, and the average throughput in the network.

3.5 | Experimental setup

In this research, we develop a SUMO-based simulation platform to systematically simulate and analyse mixed traffic, considering varying deployment scenarios of AVs, since the current resources of CAVs modelling are limited in microscopic simulators. The architecture of the simulation platform consists of three components: (i) scenario generation, (ii) simulation environment, and (iii) output module. For each scenario, the scenario generation tool utilizes inputs such as demand scale, PR, and OD matrix. This tool assigns trips in the traffic network based on the provided information and runs the SUMO microscopic resolution model. The CF behaviours of AVs and HDVs serve as inputs to guide vehicles movement and interactions within the SUMO environment. For LC configurations, we maintain the default settings of SUMO for both AVs and HDVs. Considering the stochasticity in microscopic simulations, we aggregate the outputs (i.e. evaluation indicators) over multiple simulation runs. The study area covers the traffic network of Munich city center as shown in Figure 5, which includes urban road types with morning peak-hour traffic demand. The OD pairs are allocated using a trip-based stochastic user route choice assignment.

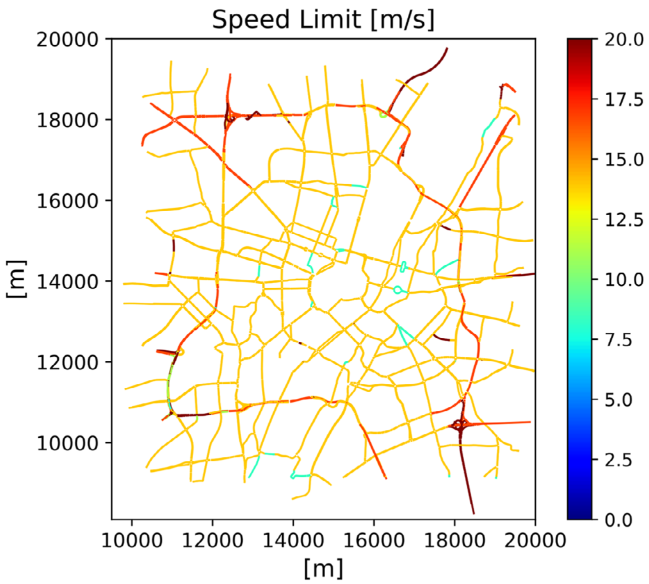

FIGURE 5 Transport network of Munich city center.

TABLE 5 IDM model's parameters range and calibrated values.

Parameters	Unit	Range of values	Calibrated value
Mingap	[m]	0.5–2.0	1.2
Accel	[m/s^2]	1.5–2.5	2.3
Decel	[m/s^2]	2.5–3.5	2.6
Tau	[s]	0.5–1.5	1.0

Meanwhile, as discussed in Section 3.2, we use IDM to calibrate the base model. The definition of the range of each parameter is necessary for the search space of the PSO. Hence, the range of each parameter of the IDM is assumed to replicate realistic driving behaviour and include the vehicle's capabilities in terms of acceleration and deceleration, as well as the comfort driving characteristics. The result of the calibration process, considering 12 simulation runs for each PSO iteration and a 15-min warm-up time is depicted in Table 5.

Additionally, in this research, we conduct impact assessment under different scenarios varying by demand fluctuations and PRs. We examine the simulation platform with two demand cases, namely, 30% below peak hour traffic and peak hour traffic demand. For each demand scale, we investigate scenarios with 0 to 100% PRs with 20% increments. Considering the overall scenario space for each demand scale, a total of 5 scenarios for AVs are generated. Meanwhile, to account for the inherent stochastic nature of microscopic simulations, we execute each scenario a total of 12 times. The resulting KPIs values are derived from the mean of all 12 simulation runs. Additionally, a 15-min warm-up period is implemented, during which no data are collected. In total, 12 scenarios (including 0% PR of AV) are executed, leading to a cumulative 144 simulation runs (12 runs for each of the 12 scenarios).

4 | RESULTS

The results section of this paper is structured into three segments. The first part describes the influences of AVs on traffic efficiency. It discusses the specific mobility effects of different AV PRs on links, intersections and overall network. The second part reveals the findings of safety assessments conducted across diverse scenarios within the Munich city network. Lastly, we present the outcomes of statistical analysis of the travel time- and conflicts-based regression models.

4.1 | Traffic efficiency

To explore the effects of different AV deployment scenarios on traffic efficiency, we employ a range of KPIs depending on the assessment area. For assessing the impacts on the overall network, we consider KPIs such as average network travel time, average waiting time, number of stops per vehicle throughout the trip, and mean time loss per vehicle. The average waiting time per vehicle is defined as the duration when the speed of a vehicle is less than 0.1 m/s, while the mean time loss per vehicle represents the time during which a vehicle operates below the ideal speed. Additionally, to investigate impacts on intersections, we use average time loss per vehicle and average intersection passing speed as indicators.

Analysing the mean network travel time in each AV scenario and comparing it with a fully HDV environment reveals a slight increase in average network time up to 40% AV PRs. Beyond this point, there is a reduction in travel time, as illustrated in Figure 6a. The results of the ANOVA test indicate that the F-value (5.741) for all AV scenarios under base demand exceeds the critical F-value (3.856) at a 95% confidence interval. This holds true for 30% below demand, where the F-value (5.506) for all AV scenarios, including 0% PR, surpasses the F-critical value (3.856). While the one-way ANOVA test reports different means among AV PRs for both demand scales, the Tukey HSD test demonstrates statistically significant changes between a fully HDV environment (0% PR) and (20%, 40%, and 60% PRs), as well as among (20%, 40% PRs) and a fully AV environment (100% PR) under the 30% below demand scale. With the base demand, only (20% and 40% PRs) exhibit significant differences from 0% PR and 100% PR.

As illustrated in Figure 6a, when the AV PRs range from 20% to 40%, the average network travel time experiences an approximately 10% increase compared to a fully HDV environment under both demand scales. This rise is primarily attributed to the behavioural changes of AVs in the network, leading to additional delays throughout the system. However, as the AV PR increases beyond 40% up to 100%, there is a subsequent reduction in average travel time, approaching levels comparable to a fully HDV scenario. This trend is consistent across other KPIs, as depicted in Figure 6b–d. This suggests that AVs do not substantially alter the overall network performance, as various influencing factors such as infrastructure, speed limits, and intersection control impose limitations on the effects of behavioural changes among vehicles in the network.

Similarly, the results of AVs impacts on the state of intersections reveal that the change in average time loss per vehicle per intersection with different AV PRs is not significantly different when compared to a fully HDVs scenario, as depicted in Figure 7. This outcome is attributed to the unchanged controlling algorithms of the traffic signals within the study area. In addition, the average passing speed per intersection remains almost the same for all AV scenarios. Hence, the behavioural difference in AVs driving configuration may not lead to substantial changes in both the mean time loss per vehicle and the average passing speed per intersection.

4.2 | Traffic safety

We use the total number of conflicts as the KPI to analyse the potential safety implications of AV PRs in the study area. A conflict is identified when the TTC value between two vehicles is less than or equal to a specific threshold set at 1.5 s in this study. Additionally, we vary the TTC threshold values for conflicts involving AV-AV and HDV interactions to explore the influence of AVs' sensing capabilities on the overall number of conflicts. This approach provides insight into how safety is affected by different AV PRs and the varying thresholds for conflict detection.

The summary statistics for traffic conflicts at different PRs of AVs are presented in Table 6, encompassing mean, minimum, and maximum values, as well as standard deviation. Initial findings indicate that, under both demand scales, increasing the PR of AVs up to 40% results in a concurrent increase in the total number of conflicts. This increase is directly linked to the distinct driving behaviour of AVs. Although in small PRs, the driving behaviour of AVs is influenced by HDVs, the change in parameters of the CF model results in a higher number of conflicts. This could also be expected in real-world scenarios where a limited PR of AVs might impact the driving behaviour of HDVs, prompting frequent adjustments in CF behaviour. Similarly, by increasing the PRs of AVs from 40% onward, there is a notable reduction in total number of conflicts. In a fully AV scenario, the total number of conflicts is around 25% lower than in a fully HDV environment. This indicates that

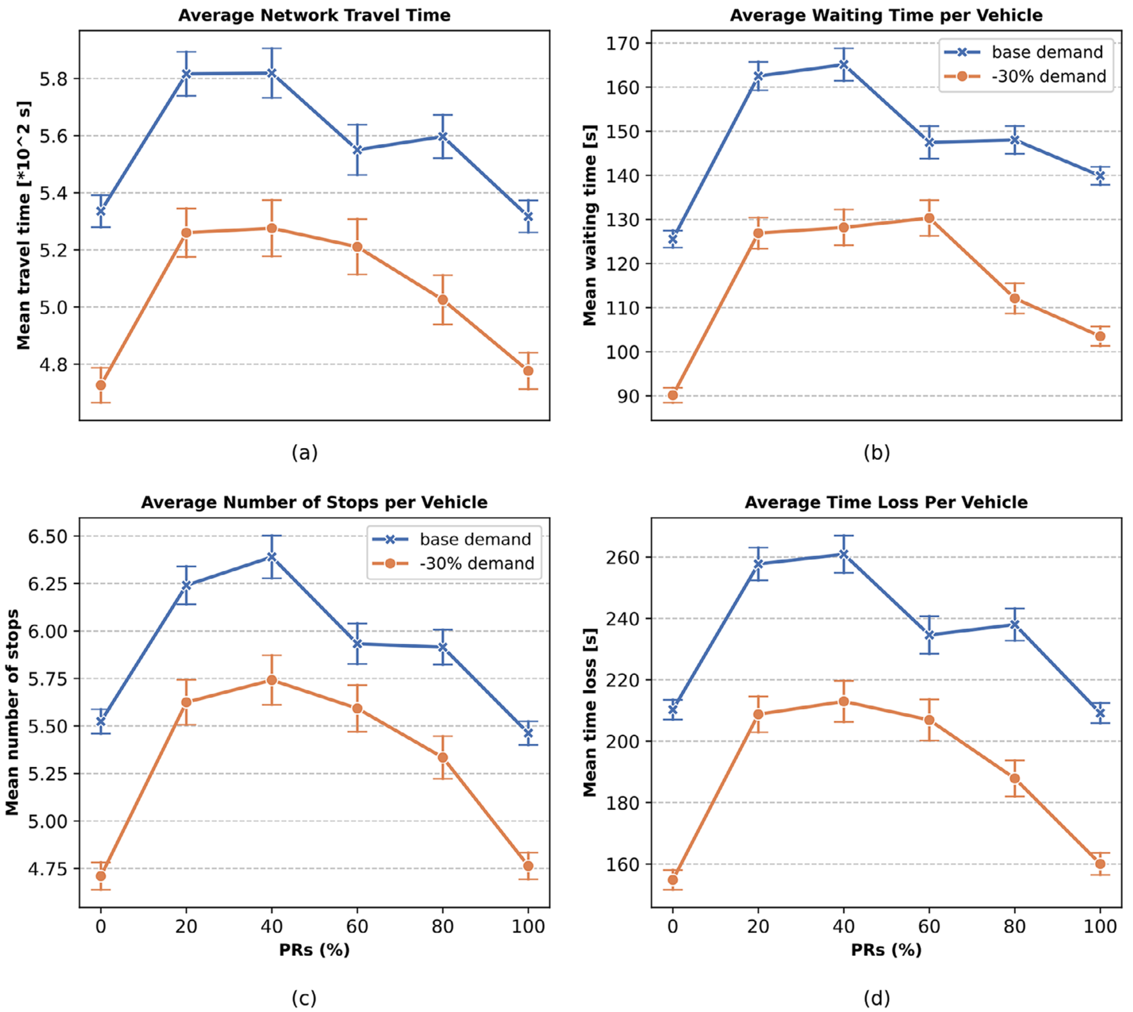

FIGURE 6 The impacts of AV PRs on (a) average network travel time, (b) average waiting time per vehicle, (c) mean number of stops per vehicle, and (d) average time loss per vehicle (the error bars show the variability of data around the mean).

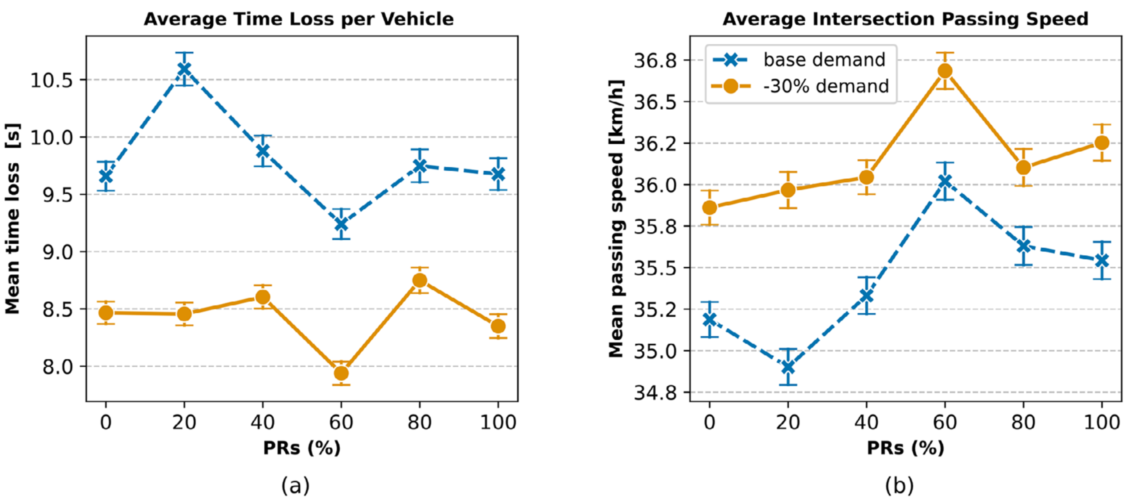

FIGURE 7 Illustration of the potential impacts of AV PRs on (a) average time loss per vehicle per intersection, and (b) average intersection passing speed (the error bars show the variability of data around the mean).

TABLE 6 Summary statistics of traffic conflicts (TTC = 1.5 s) under different PRs and demand scales.

Demand	PRs	Mean	Minimum	Maximum	Std deviation
100 %	0%	16,455	15,575	16,517	302.38
	20%	22,154	21,970	23,836	623.51
	40%	27,661	26,422	28,689	664.93
	60%	26,586	26,298	28,294	683.35
	80%	17,985	17,410	18,660	384.31
	100%	12,413	11,653	13,157	495.63
30% below	0%	8,894	8,576	9,331	250.06
	20%	13,721	13,205	15,528	619.78
	40%	17,596	16,271	18,190	521.31
	60%	17,031	16,530	17,854	365.55
	80%	10,927	9,832	11,663	485.29
	100%	6,592	6,252	7,202	286.47

AVs' CF behaviour could significantly change safety; however, in higher PRs.

Moreover, the results of the one-way ANOVA test indicate a significant variation in the total number of conflicts across all AV deployment scenarios in both demand scales. The F-value (9.974) for all AV scenarios under base demand exceeds the critical F-value (3.911) at a 95% confidence interval. Similarly, for the 30% below demand scale, the F-value (4.493) for all AV scenarios, including 0% PR, surpasses the F-critical value (3.911). Furthermore, the Tukey HSD test reveals a significant variation between all pairs of AV PRs except for 40% and 60% PRs under both demand scales.

Meanwhile, the sensing capabilities enable AVs to react faster than HDVs in conflict situations. Therefore, it is arguable that the TTC threshold for HDVs' conflicts could be set to 1.5 s, where the HDV is the following (ego) agent either in an HDV–HDV or HDV–AV situations. However, for AV–AV and AV–HDV conflicts, we can set the TTC threshold to 1.25, 1.0, and 0.75 s. In comparison to the initial scenario, where TTC is set to 1.5 s for all conflict types (Figure 8a), the total number of conflicts is significantly lower for other TTC thresholds, as depicted in Figure 8b–d. When setting the TTC threshold to 1.25 s for AV-related conflicts, the total number of conflicts in 100% PR reduces around 61% in comparison to 0%

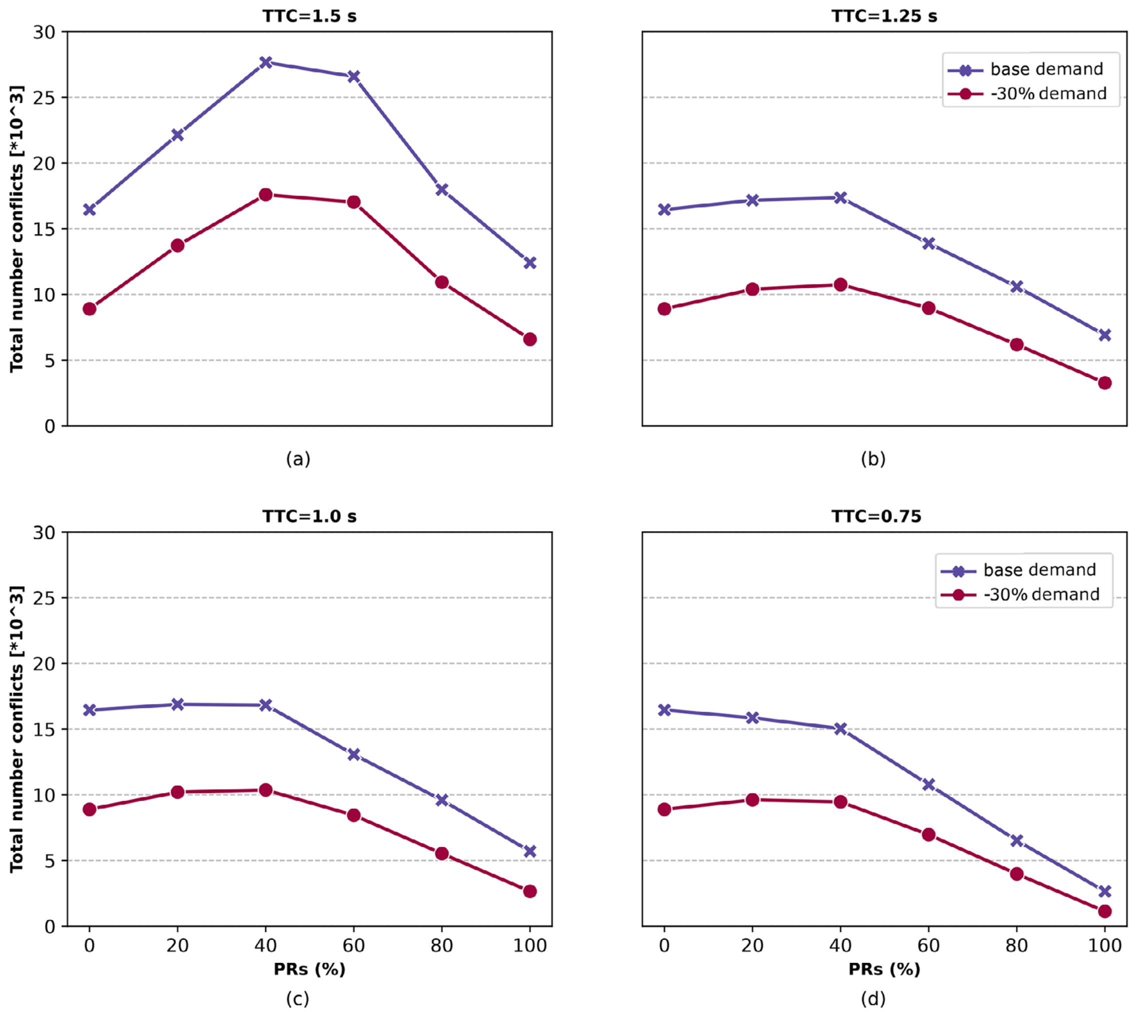

FIGURE 8 The comparison of the total number of conflicts under various TTC thresholds.

TABLE 7 The contribution of vehicle types on conflicts generation under various TTC thresholds and scenarios.

(a) TTC threshold = 1.5 s

Demand	PRs	AV-AV	AV-HDV	HDV-HDV	HDV-AV	Sum
100%	0%	0	0	16,455	0	16,455
	40%	7,214	7,109	6,218	7,120	27,661
	80%	10,328	3,220	1,259	3178	17,985
	100%	12,413	0	0	0	12,413
30% below	0%	0	0	8,894	0	8,894
	40%	4,683	4,429	4,003	4,481	17,596
	80%	6,169	2,022	846	1,890	10,927
	100%	6,592	0	0	0	6,592

(b) TTC threshold = 1.25 s

Demand	PRs	AV-AV	AV-HDV	HDV-HDV	HDV-AV	Sum
100%	0%	0	0	16,455	0	16,455
	40%	1,721	2,305	6,218	7,120	17,364
	80%	4,562	1,589	1,259	3,178	10,588
	100%	6,914	0	0	0	6,914
30% below	0%	0	0	8,894	0	8,894
	40%	950	1,312	4,003	4,481	10,746
	80%	2,480	966	846	1,890	6,182
	100%	3,264	0	0	0	3,264

(c) TTC threshold = 1.0 s

Demand	PRs	AV-AV	AV-HDV	HDV-HDV	HDV-AV	Sum
100%	0%	0	0	16,455	0	16,455
	40%	1,508	1,986	6,218	7,120	16,832
	80%	3,787	1,376	1,259	3,178	9,600
	100%	5,704	0	0	0	5,704
30% below	0%	0	0	8,894	0	8,894
	40%	782	1,109	4,003	4481	10,375
	80%	1,980	812	846	1,890	5,528
	100%	2,651	0	0	0	2,651

(d) TTC threshold = 0.75 s

Demand	PRs	AV-AV	AV-HDV	HDV-HDV	HDV-AV	Sum
100%	0%	0	0	16,455	0	16,455
	40%	707	993	6,218	7,120	15,038
	80%	1,515	569	1,259	3,178	6,521
	100%	2,648	0	0	0	2,648
30% below	0%	0	0	8,894	0	8,894
	40%	408	577	4,003	4,481	9,469
	80%	816	424	846	1,890	3,976
	100%	1,126	0	0	0	1,126

PR under both demand scenarios, where for TTC threshold 1.0 and 0.75 s, these figures show approximately 67% and 85%, respectively.

In addition, to gain a deeper understanding of the contribution of vehicle types in generating conflicts in the network, we distinguish AV and HDV-related conflicts under each TTC threshold, AV PR, and demand scale scenarios. As shown in Table 7, when setting the TTC threshold to 1.5 s, AV-related conflicts (AV-AV and AV-HDV) are higher than HDV-related conflicts under 40% PRs for both demand scenarios. The selection of a 40% PR allows us to assess the contribution of AV conflicts in a scenario where the presence of HDVs in the network is predominant. However, for lower TTC thresholds, the contribution of HDV-related conflicts is higher under 40% PR for both demand scale scenarios.

4.3 | Regression analysis

To better investigate the potential benefits of AV PRs on traffic efficiency and safety, we implement GEE and ZTP regression models, respectively, to relate the impacts with the influencing factors. For the GEE model, we use edge travel time per kilometre as a dependent variable and AV PRs, flow, length of edge, flows, and speed limit as independent variables. Whereas for the ZTP regression model, the total number of conflicts is set to the dependent variable, AV PRs, flow, and standard deviation of speed as independent variables.

4.3.1 | Travel time regression analysis

The results of the regression model with two correlation structures (independent and exchangeable) are shown in Table 8. For comparison of model goodness of fit under different correlation structures, we also use the AIC (Akaike Information Criterion) parameter (the lower value of AIC indicates a better model fit). As depicted in Table 8, the value of AIC is smaller for the independent working correlation structure, making it a better fit compared to the exchangeable correlation structure. In addition, there are differences in the coefficient and standard errors of the variables in both working correlation structures. For instance, the variable AV60 (60% PR of AV) is significant (p-value = 0.001) under the independent correlation structure, whereas it is not statistically significant (p-value = 0.132) under the exchangeable correlation structure. Meanwhile, the value of the estimated correlation matrix in the exchangeable structure is 0.754.

The investigation of the coefficient estimates of AV PRs reveals that under the independent structure, AV20, AV40, and AV80 are significant in changing edge travel time per kilometre, whereas under the exchangeable correlation structure, only AV20 and AV40 are statistically significant. The positive sign of the coefficients indicates that any AV PR increases the edge travel time per kilometre compared to a fully HDV environment; however, the magnitude of this increase is different in each AV PR. In a mixed environment, where AVs interact with HDVs, there might be frequent driving behaviour adjustments

TABLE 8 Regression-based edge travel time per kilometre analysis.

	Independent				Exchangeable			
Variable	Coeff.	Std. Err.	z value	$Pr(>\|z\|)$	Coeff.	Std. Err.	z value	$Pr(>\|z\|)$
Intercept	18.004**	3.753	4.797	<0.001	12.263**	3.845	3.189	0.001
AV20	0.931**	0.250	3.717	<0.001	0.531**	0.224	3.265	0.001
AV40	1.178**	0.277	4.262	<0.001	0.633**	0.292	2.166	0.030
AV60	0.913**	0.268	3.410	0.001	0.367	0.244	1.507	0.132
AV80	0.455	0.257	1.772	0.076	0.036	0.218	0.167	0.867
AV100	0.086	0.237	0.362	0.717	−0.289	0.180	−1.609	0.108
Edge length	0.068**	0.001	58.005	<0.001	0.071**	0.002	41.448	<0.001
Flow	0.014**	0.003	5.078	<0.001	0.030**	0.006	4.872	<0.001
Speed limit	−0.948**	0.274	−3.464	0.001	−0.765**	0.254	−3.016	0.003
AIC	500645.98				505287.27			

**Significance at 0.05 level.

toward safe manoeuvres, and this may lead to increased edge travel time per kilometre. In lower PRs, there is less driving behaviour oscillation compared to a fair share of both AVs and HDVs (e.g. 50%). Similarly, in higher PRs, the driving behaviour is influenced by AVs, and therefore, the driving actions are less disturbed for both AVs and HDVs compared with a 50% PR. As depicted in Table 8, under the independent correlation structure, the coefficient estimates of AV PR initially increase from 0.931 (AV20) to 1.178 (AV40) and then reduces gradually to 0.086 (AV100). Meanwhile, compared to the base scenario (0% PR), the travel time value per kilometre is higher in a fully AV environment (100% PR); however, the coefficient estimate is not significant, and thus, the safe driving behaviour of AVs could potentially improve safety without deteriorating traffic efficiency.

Furthermore, traffic flow significantly affects edge travel time per kilometre under both correlation structures. The higher flow results in increased travel time per kilometre. Similarly, the coefficient estimate of the speed limit is negative, which indicates that the travel time per kilometre at an urban road with higher speed limit is less compared to the same urban road with lower speed limit.

4.3.2 | Conflicts regression analysis

The findings of the conflicts-based regression model are presented in Table 9. Based on the estimated coefficients, AV PRs (except AV80) are found to be significant in affecting the total number of conflicts in the network. The signs of AV20, AV40, and AV60 are positive, whereas AV80 and AV100 have negative signs. The differences in the driving behaviour of AVs and HDVs result in increased conflicting situations. The higher the interactions among AVs and HDVs, the higher is the total number of conflicts. In scenarios with both low and high AV PRs, the total number of conflicts tends to be lower compared to situations with an equal mix of AVs and HDVs (e.g. 50% AV PR). In lower PRs, the number of conflicts tends to be like the fully HDV scenario since the driving behaviour of AVs is influenced by HDVs. Similarly, in higher PRs, the number of conflicts is associated to AVs and tends toward a fully AV scenario. By increasing the PR up to 50%, the total number of conflicts increases, where with higher PRs (>50%), the change in the total number of conflicts in comparison to a fully HDV scenario reduces. When the PR reaches 80%, the change in the total number of conflicts compared to the based scenario is insignificant. However, in a 100% PR, the total number of conflicts reduces significantly. Therefore the coefficient estimates increase from 0.044 (AV20) to 0.124 (AV40), and then reduces to −0.008 (AV80) and finally to −0.695 (AV100).

TABLE 9 Regression-based conflicts analysis.

Variable	Coeff.	Std. Err.	z value	$Pr(>\|z\|)$
Intercept	2.484**	0.058	42.740	<0.001
AV20	0.044**	0.010	4.237	<0.001
AV40	0.124**	0.010	11.924	<0.001
AV60	0.074**	0.011	6.676	<0.001
AV80	−0.001	0.011	−0.077	0.939
AV100	−0.695**	0.022	−31.590	<0.001
Log (flow)	0.305**	0.005	60.739	<0.001
Speed Std	0.142**	0.003	43.078	<0.001

**Significance at 0.05 level.

Additionally, the standard deviation of speed is a significant variable in changing the total number of conflicts in the network. Higher fluctuation in this variable results in higher conflicts. Meanwhile, the increased traffic flow (throughput) in the network implies higher conflicts in the network.

5 | DISCUSSION

The findings of the literature review revealed that most simulation-based AV studies conduct the impact assessment on traffic efficiency [18, 21, 22, 30, 34, 35, 66], safety [17, 22, 28, 32, 55], and some also focus on environmental effects [24, 25, 75]. Regarding the mobility impacts, researchers reported that higher PRs of AVs and CAVs reduce travel time and increase capacity and throughput [17, 18, 21, 22, 33]. However, other studies claimed that in a mixed driving environment where AVs interact with HDVs, the capacity degrades [19, 34], and travel time increases [66]. In addition, it is reported that in higher speed limits, the impact of AVs on Freeway capacity is significant. In contrast, in lower speed limits, the change is not considerable [35]. Meanwhile, most studies reported that CAVs outperform AVs in many aspects due to their communication capabilities. For instance, [22] reported that at least 20% PR of CAVs is required to significantly reduce travel time, whereas, for AVs, at least 40% PR is required. On the other hand, the results of our research show that a mixed environment of AVs and HDVs increases the network travel time, vehicle time loss, and average flow. Second, regarding safety impacts, most studies suggested that by increasing the PR of AVs, the total number of conflicts in the network reduces significantly [17, 22, 32, 55]. Some also highlighted the negative impacts of AVs on roundabout safety [64]. However, our research revealed that a comparable mix of AVs and HDVs might result in an increased number of conflicts. Since different driving behaviours of AVs and CAVs may lead to the frequent adjustment of driving actions, the number of conflicts increases. However, with higher PRs of AVs (e.g. more than 80%), the total number of conflicts significantly reduces in comparison to a fully HDV environment. With 100% AV PR, the total number of conflicts decreases by around 25%. The inconsistent conclusion on the impacts of AV PRs could be associated with two main influencing factors: the assumption on the potential CF parameters of AVs driving behaviour and the scope of the study.

The driving behaviour of AVs might significantly differ from HDVs. In MTMs, the driving behaviour of AVs is distinguished from HDVs by modifying the parameters of the CF model. However, the magnitude of these changes depends on the researchers' own assumptions (due to the lack of large real-world data for AVs). Most studies, for instance, assume that AVs might drive closer to the leading vehicles and could react relatively faster. However, AVs may have more cautious behaviour and strictly follow the traffic rules, especially the speed limits, compared to HDVs. Therefore, in this research, we utilize AVs' optimized and safe driving behaviour instead of assuming the CF model parameters.

Another important aspect is the scope of the study. Most studies conduct the impact assessment on freeways and highways, where the fluctuation of traffic flow elements is not huge. Thus, AV driving behaviour brings a significant change in efficiency and safety. In contrast, in an urban network, many other influencing factors such as the type of roads, number of lanes, type and number of intersections, curvatures, control devices, speed limits, and more could have direct impacts on the driving performance and impress the potential effects of driving behaviour itself. In other words, these influential factors could diminish the effects of AV driving behaviour on traffic efficiency. Therefore, in this research, the findings differ for efficiency evaluation. A similar result is also reported by [66], where the investigation is conducted at the network level. On the other hand, regarding safety, driving behaviour significantly affects the number of conflicts. Since a conflict occurs between two vehicles (following and leading) in a short period and is unrelated to the entire vehicle's trip, the driving behaviour is responsible for any possible conflict.

6 | CONCLUSION

It is expected that AVs have a different driving behaviour than HDVs. This behavioural difference might bring a significant change in mobility, safety, and emissions. Identification of the potential driving behaviour of AVs is a crucial aspect of impact assessment studies. Since AVs might have safe and efficient driving behaviour, a simulation-based impact assessment with optimal driving behaviour of AVs might report more realistic results on the potential impacts of AVs. Hence, in this research, we conduct a comprehensive simulation-based impact assessment under varying scenarios to evaluate the effects of AVs on efficiency and safety in an urban network. An experimental setup is conducted to run the simulations in the Munich city network. We utilize Krauss and IDM models to mimic the CF behaviour of AVs and HDVs, respectively. The parameter of the HDV CF model is calibrated using PSO algorithm, whereas for the Krauss model, the optimized parameters are used from another study.

The evaluation of impacts on traffic efficiency reveals that any PR of AVs might increase the network travel time under various demand scenarios. This increase is mainly due to the behavioural changes of vehicles in mixed environments. With 20–40% PRs, the results show around 10% increase in travel time, where this figure reduces gradually for PRs ranging from 40% to 100%. In a fully AV scenario, the network travel time is almost the same as in the base scenario (0% PR). The same findings are found for other KPIs, including the average number of stops per vehicle, average time loss per vehicle, and average time loss per vehicle per intersection. Hence, behavioural differences in AV driving configurations could not bring huge changes on traffic efficiency in urban networks. On the other hand, the analysis of traffic safety depicts that by increasing the PRs of AVs to 40%, the total number of conflicts (with TTC <1.5 s) increases significantly; however, with higher PRs, the number of conflicts reduces significantly. In addition, it is found that the total number of conflicts is around 25% less in a fully AV environment in comparison to the base scenario. Meanwhile, if we consider the sensing capabilities of AVs for their fast reaction in case of a conflict situation, the total number of conflicts in the network reduces significantly by increasing the PRs of AVs. Depending on the TTC value for AV-related conflicts (AV to AV or AV to HDV), the total number of conflicts reduces around 60 to 80% in higher PRs (>80%).

The investigation of the potential impacts of AVs showed that AVs might bring safety improvement not only by eliminating the drivers' errors but also by their behavioural changes; however, their impacts on efficiency in a city network scale, where additional infrastructure-related factors (e.g. speed limit, type of roads, number of lanes, type of intersections, traffic control devices, and more) play a vital role is not huge. This research also has limitations that could raise new lines of work for further studies. First, for any PR of AVs, we fixed the driving behaviour of HDVs; however, the mass deployment of AVs might also change the behaviour of HDVs and their interaction with AVs. Thus, a research using a driving simulator experiment of the field test is required to evaluate the potential change in human drivers' behaviour when interacting with AVs and utilize these changes when conducting impact assessment. This will lead to more accurate and reliable findings on AVs impact assessment. Second, in an urban network, among other influential factors, speed limit could have a major contribution in diminishing the real impacts caused by behavioural changes in driving. Hence, a sensitivity analysis of different speed limit policies could be valuable research work to investigate the relationship between speed limits and the potential impacts of AVs on efficiency and safety. Third, in simulation-based studies, the effects of AVs are influenced by factors such as the selection of CF models and the scope of the study. Therefore, it is important to perform a sensitivity analysis using varying modelling techniques to find the interactions among a CF model and the potential impacts and to analyse the relationship between the scope of a study and the impacts of AVs deployment scenarios. Fourth, in this research, we utilized the optimized driving behaviour of AVs (extracted in a city network) to conduct an impact assessment. However, it is interesting to study the impacts of AVs on a freeway or highway by utilizing the AVs' optimal driving behaviour. The aim would be to evaluate the effects of optimal driving behaviour of AVs under high speed and traffic flow. Finally, there is a potential to integrate a data-driven model into a microscopic traffic simulator to replicate the driving behaviour of AVs under varying traffic conditions and conduct impact assessment. This will generate plausible findings on the potential impacts of AVs in mixed traffic.

AUTHOR CONTRIBUTIONS

Hashmatullah Sadid: Conceptualization; formal analysis; methodology; validation; visualization; writing—original draft. **Constantinos Antoniou**: Conceptualization; funding acquisition; supervision; writing—review & editing.

ACKNOWLEDGEMENTS

This study was funded by Deutscher Akademischer Austauschdienst (DAAD), Research Grants – Doctoral Programmes in Germany.

Open access funding enabled and organized by Projekt DEAL.

CONFLICT OF INTEREST STATEMENT

The authors declare no conflicts of interest.

DATA AVAILABILITY STATEMENT

The data that support the findings of this study are available from the corresponding author upon reasonable request.

ORCID

Hashmatullah Sadid https://orcid.org/0000-0002-5577-2468

Constantinos Antoniou https://orcid.org/0000-0003-0203-9542

REFERENCES

1. Yue, L., Abdel-Aty, M., Wu, Y., Wang, L.: Assessment of the safety benefits of vehicles advanced driver assistance, connectivity and low level automation systems. Accid. Anal. Prev. 117, 55–64 (2018)
2. Shladover, S.E.: Cooperative (rather than autonomous) vehicle-highway automation systems. IEEE Intell. Transp. Syst. Mag. 1(1), 10–19 (2009)
3. Fagnant, D.J., Kockelman, K.: Preparing a nation for autonomous vehicles: Opportunities, barriers and policy recommendations. Transp. Res. Part A: Policy Pract. 77, 167–181 (2015)
4. Chen, Y., Gonder, J., Young, S., Wood, E.: Quantifying autonomous vehicles national fuel consumption impacts: a data-rich approach. Transp. Res. Part A: Policy Pract. 122, 134–145 (2019)
5. Stern, R.E., Chen, Y., Churchill, M., Wu, F., Monache, M.L.D., Piccoli, B., Seibold, B., Sprinkle, J., Work, D.B.: Quantifying air quality benefits resulting from few autonomous vehicles stabilizing traffic. Transp. Res. Part D: Transp. Environ. 67, 351–365 (2019)
6. Ma, J., Hu, J., Leslie, E., Zhou, F., Huang, P., Bared, J.: An eco-drive experiment on rolling terrains for fuel consumption optimization with connected automated vehicles. Transp. Res. Part C: Emerging Technol. 100, 125–141 (2019)
7. Rahman, M.M., Deb, S., Strawderman, L., Burch, R., Smith, B.: How the older population perceives self-driving vehicles. Transp. Res. Part F: Traffic Psychol. Behav. 65, 242–257 (2019)
8. Marczuk, K., Soh, H., Azevedo, C.L., Adnan, M., Pendleton, S., Frazzoli, E., Lee, D.: Autonomous mobility on demand in SimMobility: case study of the central business district in Singapore. In: 2015 IEEE 7th International Conference on Cybernetics and Intelligent Systems (CIS) and IEEE Conference on Robotics, Automation and Mechatronics (RAM), pp. 167–172. IEEE, Piscataway, NJ (2015)
9. Banks, V.A., Plant, K.L., Stanton, N.A.: Driver error or designer error: using the perceptual cycle model to explore the circumstances surrounding the fatal Tesla crash on 7th May 2016. Saf. Sci. 108, 278–285 (2018)
10. Taeihagh, A., Lim, H.S.M.: Governing autonomous vehicles: emerging responses for safety, liability, privacy, cybersecurity, and industry risks. Transp. Rev. 39(1), 103–128 (2019)
11. Bansal, P., Kockelman, K.M., Singh, A.: Assessing public opinions of and interest in new vehicle technologies: an Austin perspective. Transp. Res. Part C: Emerging Technol. 67, 1–14 (2016)
12. Litman, T.: Autonomous Vehicle Implementation Predictions: Implications for Transport Planning. The National Academies of Sciences, Engineering, and Medicine, Washington, D.C. (2022)
13. Othman, K.: Public Transportation on the Era of Autonomous Vehicles: Exploring Different Scenarios. Civil Eng. Res. J. 10(5), 15–16 (2020)
14. Amini, R.E., Katrakazas, C., Riener, A., Antoniou, C.: Interaction of automated driving systems with pedestrians: challenges, current solutions, and recommendations for eHMIs. Transp. Rev. 41(6), 788–813 (2021)
15. Do, W., Rouhani, O.M., Miranda-Moreno, L.: Simulation-based connected and automated vehicle models on highway sections: a literature review. J. Adv. Transp. 2019, 1–14 (2019)
16. Talebpour, A., Mahmassani, H.S.: Influence of connected and autonomous vehicles on traffic flow stability and throughput. Transp. Res. Part C: Emerging Technol. 71, 143–163 (2016)
17. Karbasi, A., O'Hern, S.: Investigating the impact of connected and automated vehicles on signalized and unsignalized intersections safety in mixed traffic. Future Transp. 2(1), 24–40 (2022)
18. Cao, Z., Lu, L., Chen, C., Chen, X.: Modeling and simulating urban traffic flow mixed with regular and connected vehicles. IEEE Access 9, 10 392–10 399 (2021)
19. Carrone, A.P., Rich, J., Vandet, C.A., An, K.: Autonomous vehicles in mixed motorway traffic: capacity utilisation, impact and policy implications. Transportation 48(6), 2907–2938 (2021)
20. Olia, A., Razavi, S., Abdulhai, B., Abdelgawad, H.: Traffic capacity implications of automated vehicles mixed with regular vehicles. J. Intell. Transp. Syst. 22(3), 244–262 (2018)

21. Ma, X., Hu, X., Weber, T., Schramm, D.: Effects of automated vehicles on traffic flow with different levels of automation. IEEE Access 9, 3630–3637 (2021)
22. Rahman, M.H., Abdel-Aty, M., Wu, Y.: A multi-vehicle communication system to assess the safety and mobility of connected and automated vehicles. Transp. Res. Part C: Emerging Technol. 124, 102887 (2021)
23. Li, H., Li, W.: Estimating the average road travel time based on soft set under connected and autonomous vehicles. In: 2020 5th International Conference on Information Science Computer Technology and Transportation (ISCTT), pp. 566–570. IEEE, Piscataway, NJ (2020)
24. Makridis, M., Mattas, K., Mogno, C., Ciuffo, B., Fontaras, G.: The impact of automation and connectivity on traffic flow and CO2 emissions. a detailed microsimulation study. Atmos. Environ. 226, 117399 (2020)
25. Mattas, K., Makridis, M., Hallac, P., Raposo, M.A., Thiel, C., Toledo, T., Ciuffo, B.: Simulating deployment of connectivity and automation on the Antwerp ring road. IET Intel. Transp. Syst. 12(9), 1036–1044 (2018)
26. Makridis, M., Mattas, K., Ciuffo, B., Raposo, M.A., Toledo, T., Thiel, C.: Connected and automated vehicles on a freeway scenario. Effect on traffic congestion and network capacity. In: Proceedings of 7th Transport Research Arena TRA 20, pp. 1–10. Zenodo, Geneva (2018)
27. Kim, B., Heaslip, K.P., Aad, M.A., Fuentes, A., Goodall, N.: Assessing the impact of automated and connected automated vehicles on Virginia freeways. Transp. Res. Rec.: J. Transp. Res. Board 2675(9), 870–884 (2021)
28. Miqdady, T., de Oña, R., Casas, J., de Oña, J.: Studying traffic safety during the transition period between manual driving and autonomous driving: a simulation-based approach. IEEE Trans. Intell. Transp. Syst. 24(6), 6690–6710 (2023)
29. Song, H., Zhao, F., Zhu, G., Liu, Z.: Impacts of connected and autonomous vehicles with level 2 automation on traffic efficiency and energy consumption. J. Adv. Transp. 2023, 1–15 (2023)
30. Tympakianaki, A., Nogues, L., Casas, J., Brackstone, M., Oikonomou, M.G., Vlahogianni, E.I., Djukic, T., Yannis, G.: Autonomous vehicles in urban networks: a simulation-based assessment. Transp. Res. Rec. 2676(10), 540–552 (2022)
31. Sadid, H., Qurashi, M., Antoniou, C.: Simulation-based optimization of autonomous driving behaviors. In: 2022 IEEE 25th International Conference on Intelligent Transportation Systems (ITSC), pp. 4101–4108. IEEE, Piscataway, NJ (2022)
32. Morando, M.M., Tian, Q., Truong, L.T., Vu, H.L.: Studying the safety impact of autonomous vehicles using simulation-based surrogate safety measures. J. Adv. Transp. 2018, 1–11 (2018)
33. Lu, Q., Tettamanti, T.: Impacts of autonomous vehicles on the urban fundamental diagram. In: Fifth International Conference on Road and Rail Infrastructure, pp. 1265–1271. International Road Federation, Geneva (2018)
34. Shang, M., Stern, R.E.: Impacts of commercially available adaptive cruise control vehicles on highway stability and throughput. Transp. Res. Part C: Emerging Technol. 122, 102897 (2021)
35. Liu, P., Fan, W.D.: Exploring the impact of connected and autonomous vehicles on freeway capacity using a revised intelligent driver model. Transp. Plann. Technol. 43(3), 279–292 (2020)
36. Liu, H., Kan, X.D., Shladover, S.E., Lu, X.-Y., Ferlis, R.E.: Modeling impacts of cooperative adaptive cruise control on mixed traffic flow in multi-lane freeway facilities. Transp. Res. Part C: Emerging Technol. 95, 261–279 (2018)
37. Gazis, D.C., Herman, R., Rothery, R.W.: Nonlinear follow-the-leader models of traffic flow. Oper. Res. 9(4), 545–567 (1961)
38. Gipps, P.G.: A behavioural car-following model for computer simulation. Transp. Res. Part B: Methodol. 15(2), 105–111 (1981)
39. Treiber, M., Hennecke, A., Helbing, D.: Congested traffic states in empirical observations and microscopic simulations. Phys. Rev. E 62(2), 1805–1824 (2000)
40. Bando, M., Hasebe, K., Nakayama, A., Shibata, A., Sugiyama, Y.: Dynamical model of traffic congestion and numerical simulation. Phys. Rev. E 51(2), 1035–1042 (1995)
41. Wiedemann, R.: Simulation des Strassenverkehrsflusses. Springer, Wiesbaden (1974)
42. He, L., Wang, X.: Calibrating car-following models on urban streets using naturalistic driving data. J. Transp. Eng. Part A: Syst. 149(4) (2023)
43. Zheng, S.-T., Jiang, R., Tian, J., Li, X., Treiber, M., Li, Z.-H., Gao, L.-D., Jia, B.: Empirical and experimental study on the growth pattern of traffic oscillations upstream of fixed bottleneck and model test. Transp. Res. Part C: Emerging Technol. 140, 103729 (2022)
44. Zhou, X., Wang, Z., Cosio, A., Wang, J.: Parameterized derivative-free optimization approach for car-following model calibration. IFAC-PapersOnLine 54(20), 876–881 (2021)
45. Yu, M., (David)Fan, W.: Calibration of microscopic traffic simulation models using metaheuristic algorithms. Int. J. Transp. Sci. Technol. 6(1), 63–77 (2017)
46. Li, L., Chen, X.M., Zhang, L.: A global optimization algorithm for trajectory data based car-following model calibration. Transp. Res. Part C: Emerging Technol. 68, 311–332 (2016)
47. Kesting, A., Treiber, M.: Calibrating car-following models by using trajectory data: methodological study. Transp. Res. Rec.: J. Transp. Res. Board 2088(1), 148–156 (2008)
48. Liu, Z., Yang, G.: Large-scale traffic flow simulation based on intelligent pso. MATEC Web Conf. 355, 02010 (2022)
49. Aghabayk, K., Sarvi, M., Young, W.: Including heavy vehicles in a car-following model: modelling, calibrating and validating. J. Adv. Transp. 50(7), 1432–1446 (2016)
50. Daguano, R.F., Yoshioka, L.R., Netto, M.L., Marte, C.L., Isler, C.A., Santos, M.M.D., Justo, J.F.: Automatic calibration of microscopic traffic simulation models using artificial neural networks. Sensors 23(21), 8798 (2023)
51. Liu, Y., Zou, B., Ni, A., Gao, L., Zhang, C.: Calibrating microscopic traffic simulators using machine learning and particle swarm optimization. Transp. Lett. 13(4), 295–307 (2021)
52. Dadashzadeh, N., Ergun, M., Kesten, S., Žura, M.: An automatic calibration procedure of driving behaviour parameters in the presence of high bus volume. Promet - Traffic Transp. 31(5), 491–502 (2019)
53. Jiang, R., Wu, Q., Zhu, Z.: Full velocity difference model for a car-following theory. Phys. Rev. E 64, 017101 (2001)
54. Sadid, H., Antoniou, C.: Modelling and simulation of (connected) autonomous vehicles longitudinal driving behavior: a state-of-the-art. IET Intell. Transp. Syst. 17(6), 1051–1071 (2023)
55. Papadoulis, A., Quddus, M., Imprialou, M.: Evaluating the safety impact of connected and autonomous vehicles on motorways. Accid. Anal. Prev. 124, 12–22 (2019)
56. Fellendorf, M., Vortisch, P.: Microscopic traffic flow simulator VISSIM. In: Fundamentals of Traffic Simulation, pp. 63–93. Springer, New York, NY (2010)
57. Zeidler, V., Buck, H.S., Kautzsch, L., Vortisch, P., Weyland, C.M.: Simulation of autonomous vehicles based on Wiedemann's car following model in PTV Vissim. In: Conference: 98th Annual Meeting of the Transportation Research Board (TRB), pp. 1–12. Transportation Research Board, Washington, D.C. (2019)
58. Casas, J., Ferrer, J.L., Garcia, D., Perarnau, J., Torday, A.: Traffic Simulation with Aimsun. In: Fundamentals of Traffic Simulation, pp. 173–232. Springer, New York, NY (2010)
59. Krajzewicz, D.: Traffic Simulation with SUMO – Simulation of Urban Mobility. In: Fundamentals of Traffic Simulation, pp. 269–293. Springer, New York, NY (2010)
60. Krauss, S.: Microscopic modeling of traffic flow: investigation of collision free vehicle dynamics (1998)
61. Shladover, S.E., Su, D., Lu, X.-Y.: Impacts of cooperative adaptive Cruise Control on Freeway Traffic Flow. Transp. Res. Rec.: J. Transp. Res. Board 2324(1), 63–70 (2012)
62. Milanés, V., Shladover, S.E.: Modeling cooperative and autonomous adaptive cruise control dynamic responses using experimental data. Transp. Res. Part C: Emerging Technol. 48, 285–300 (2014)
63. Lu, Q., Tettamanti, T., Hörcher, D., Varga, I.: The impact of autonomous vehicles on urban traffic network capacity: an experimental analysis by microscopic traffic simulation. Transp. Lett. 12(8), 540–549 (2020)

64. Tibljaš, A.D., Giuffrè, T., Surdonja, S., Trubia, S.: Introduction of autonomous vehicles: roundabouts design and safety performance evaluation. Sustainability 10(4), 1060 (2018)
65. Aria, E., Olstam, J., Schwietering, C.: Investigation of automated vehicle effects on driver's behavior and traffic performance. Transp. Res. Proc. 15, 761–770 (2016)
66. Lu, Q.-L., Qurashi, M., Varesanovic, D., Sodnik, J., Antoniou, C.: Exploring the influence of automated driving styles on network efficiency. Transp. Res. Proc. 52, 380–387 (2021)
67. Kennedy, J., Eberhart, R.: Particle swarm optimization. In: Proceedings of ICNN'95 - International Conference on Neural Networks, vol. 4, pp. 1942–1948. IEEE, Piscataway, NJ (1995)
68. Papazoglou, G., Biskas, P.: Review and comparison of genetic algorithm and particle swarm optimization in the optimal power flow problem. Energies 16(3), 1152 (2023)
69. Wihartiko, F.D., Wijayanti, H., Virgantari, F.: Performance comparison of genetic algorithms and particle swarm optimization for model integer programming bus timetabling problem. IOP Conf. Ser.: Mater. Sci. 332(1), 012020 (2018)
70. Gad, A.G.: Particle swarm optimization algorithm and its applications: a systematic review. Arch. Comput. Methods Eng. 29(5), 2531–2561 (2022)
71. Liang, K.-Y., Zeger, S.L.: Longitudinal data analysis using generalized linear models. Biometrika 73(1), 13–22 (1986)
72. Abdi, H., Williams, L.J.: Tukey's honestly significant difference (HSD) test. In: Encyclopedia of Research Design, pp. 584–585. SAGE Publications, Inc. (2010). https://doi.org/10.4135/9781412961288
73. Plackett, R.L.: The truncated Poisson distribution. Biometrics 9(4), 485–488 (1953)
74. Hu, Y., Li, Y., Yuan, C., Huang, H.: Modeling conflict risk with real-time traffic data for road safety assessment: a copula-based joint approach. Transp. Saf. Environ. 4(3), tdac017 (2022)
75. Rios-Torres, J., Malikopoulos, A.A.: Impact of connected and automated vehicles on traffic flow. In: 2017 IEEE 20th International Conference on Intelligent Transportation Systems (ITSC), pp. 1–6. IEEE, Piscataway, NJ (2017)

How to cite this article: Sadid, H., Antoniou, C.: A simulation-based impact assessment of autonomous vehicles in urban networks. IET Intell. Transp. Syst. 18, 1677–1696 (2024). https://doi.org/10.1049/itr2.12537